Progress In Electromagnetics Research, PIER 78, 301–320, 2008

HIGH BIT RATE DENSE DISPERSION MANAGED OPTICAL COMMUNICATION SYSTEMS WITH DISTRIBUTED AMPLIFICATION

M. Mishra [†] **and S. Konar**

Department of Applied Physics
Birla Institute of Technology
Mesra-835215, Ranchi, India

Abstract—In this paper we have investigated optical pulse propagation in a dense dispersion managed (DM) optical communication system operating at a speed of 100 Gb/s and more taking into account of the effects of third order dispersion, intra-pulse Raman scattering and self steepening. Using perturbed variational formulation, we have obtained several ordinary differential equations for various pulse parameters. These equations have been solved numerically to identify launching criteria in the first DM cell of the system. Full numerical simulation of the nonlinear Schrödinger equation has been employed to identify effects of higher order terms on pulse propagation and to investigate the intra-pulse interaction. The roles played by these higher order linear and nonlinear effects have been identified. It has been found that the shift of the pulse centre due to intra-pulse Raman scattering increases with the increase in the distance of propagation and average dispersion. We have noticed that for higher value of average dispersion pulses travel less distance before collision than for lower average dispersion.

1. INTRODUCTION

Dispersion managed (DM) solitons have shown great opportunity in long distance high speed optical fiber communication systems because of their superb characteristics which are not achievable in conventional soliton based systems [1–18]. In a dispersion-managed system, fiber dispersion varies alternately between anomalous and normal values.

[†] Also with Department of Applied Sciences and Humanities, United College of Engineering and Research, Allahabad-211010, India

This variation is maintained periodically and the average dispersion over a period could be positive, negative or even zero [3, 5, 8]. Unlike in the constant dispersion system where the pulse propagates maintaining its shape unchanged, in the dispersion managed system the pulse width oscillates periodically and the shape of the pulse ranges from hyperbolic secant to Gaussian to flat top, depending on the strength of the dispersion management [4, 16]. The DM solitons have many advantages like enhanced signal to noise ratio, reduced Gordon-Haus timing jitter and the possibility of suppression of the phase matched four wave mixing processes which arises in the wavelength division multiplexing systems. The last factor could be achieved with considerable success by allowing large local dispersion [3, 15].

However, at very high transmission rate, where short pulses are required, the performance of the conventional DM soliton systems is even worse than the conventional soliton systems. In a conventional DM soliton system, where the DM period is either same as or longer than the amplifier spacing, the requirement of short pulses for high bit rate resulting in very strong dispersion management i.e., very large value of map strength due to large local dispersion. For such cases, associated increase in the pulse energy and breathing within one dispersion period lead to enhanced soliton interaction. On the other hand, short pulses in a conventional DM soliton system can be supported by keeping the map strength low enough. In fact, map strength can be made low only by reducing the magnitude of fiber dispersion, particularly, for desired low value of map strength, local dispersion approaches average dispersion. This arrangement on the other hand makes the map less effective in reducing four wave mixing impairments. Thus, to support DM solitons at a single channel bit rate higher than 60 Gb/s or more, an alternate arrangement is to use a short-period dispersion map (SPDM), where more than one DM cell of length L is fitted within one amplifier spacing L_a i.e., $L \prec\prec L_a$. In such dispersion maps the lengths of alternate dispersion sections are significantly reduced and can be chosen to keep pulse breathing and interactions small while keeping the local dispersion high enough to suppress four wave mixing impairments [19–21]. Such a scheme is also known as densely dispersion managed systems (DDMS). At high transmission rate, for example at 100 Gb/s and beyond the required pulse width (FWHM) is of the order of only a few picoseconds or less. For such cases, intrapulse Raman scattering (IRS), third order dispersion and self steeping effects can become very appreciable. In an earlier publication [22], pulse propagation incorporating stimulated Raman scattering (SRS) and third order dispersion (TOD) has been investigated. In this investigation collective variable theory (CV)

appropriate to pulse propagation in dispersion managed optical fiber link was developed. Above study was mainly confined to analyse the ability of CV treatments to accurately predict the effect of pulse interaction in wavelength division multiplexed (WDM) systems. This study was not directed to optimise the dispersion map so as to reduce the effects SRS, TOD, self steepening (ST) and cross phase modulation (XPM). However, in any DM based soliton system, the map strength parameter S is extremely important, which can be optimised to get better transmission performance. This will be undertaken in the present investigation. In the present investigation we have deliberately kept the value of S at 1.65 to get maximum transmission performance.

Therefore, in the present communication, we investigate the data transmission at 100 Gb/s and higher rate over more than 3000 km in a DM system with SPDM. For compensating fiber loss most experimental systems employ lumped amplification by placing fiber amplifier periodically along the transmission line. In order to avoid large peak power variation, which is inherent in lumped amplification scheme, we introduce distributed amplification using a bidirectional pumping scheme. The arrangement of the paper is as follows. In Section 2 we have developed the mathematical model, which is based on modified nonlinear Schrödinger equation. We have employed perturbed variational method to obtain a set of ordinary differential equations (ODE). Using periodic boundary conditions these ODE's have been solved in section 3 to find out the launching criteria of input pulses in the DDMS. In this section we have employed split step Fourier method (SSFM) to undertake full numerical simulation of the modified nonlinear Schrödinger equation. Main results have been highlighted in this section. A brief conclusion has been added in Section 4.

2. THE MODEL

The dynamics of optical pulses in a dispersion managed optical communication system is governed by the modified nonlinear Schrödinger equation (MNLSE) [23]:

$$i\frac{\partial E}{\partial z} - \frac{\beta_2(z)}{2}\frac{\partial^2 E}{\partial t^2} + \gamma|E|^2E - i\frac{\beta_3}{6}\frac{\partial^3 E}{\partial t^3} = \frac{i}{2}[g(z)-\alpha]E + \gamma\Gamma_R E\frac{\partial|E|^2}{\partial t} - \frac{i\gamma}{\omega_0}\frac{\partial\left(|E|^2E\right)}{\partial t}, \quad (1)$$

where E is the slowing varying envelop of the soliton, t is retarded time, β_2 is varying group velocity dispersion, β_3 is the third order dispersion which is assumed to be constant along fiber sections, ω_0 is the central

frequency, α accounts for the fiber loss due to absorption which is also assumed to be constant along the fiber, γ is the nonlinear coefficient responsible for self phase modulation (SPM), Γ_R is the stimulated Raman scattering coefficient. The distributed amplification of solitons is included through the gain $g(z)$.

Using following normalization $d(z) = -\frac{\beta_2 L}{T_0^2}$, $E = \sqrt{P_0}u$, $\tau = \frac{t}{T_0}$, $Z = \frac{z}{L}$, $T_R = \frac{\Gamma_R}{T_0}$, $\gamma P_0 L = 1$, $\mu = \frac{\beta_3 L}{6T_0^3}$, $\varepsilon = \frac{1}{\omega_0 T_0}$, $g'(z) = g(z)L$, $\alpha' = \alpha L$, where L is length of the dispersion map in km, T_0 is $(1/e)$ width of the optical soliton in ps and P_0 is an arbitrary characteristic power, equation (1) can be rewritten as

$$i\frac{\partial u}{\partial Z} + d(Z)\frac{\partial^2 u}{\partial \tau^2} + |u|^2 u - i\mu\frac{\partial^3 u}{\partial \tau^3} = \frac{i}{2}[g'(z) - \alpha'(Z)]u + T_R u\frac{\partial |u|^2}{\partial \tau} - i\varepsilon\frac{\partial\left(|u|^2 u\right)}{\partial \tau} \tag{2}$$

Using the transformation $u = A\sqrt{G(Z)}$, with $G(Z) = e^{\int_0^Z [g'(z)-\alpha']dz'}$ is the cumulative net gain from 0 to Z, equation (2) is now recasted as,

$$i\frac{\partial A}{\partial Z} + \frac{d(z)}{2}\frac{\partial^2 A}{\partial \tau^2} + G(Z)|A|^2 A - i\mu\frac{\partial^3 A}{\partial \tau^3} = iR, \tag{3}$$

where $R = -iT_R G(Z)A\frac{\partial |A|^2}{\partial \tau} - \varepsilon G(z)\frac{\partial(|A|^2 A)}{\partial \tau}$.

We consider a symmetric dispersion map as shown in Figure 1. The fiber dispersion is the sum of a locally varying part and an average

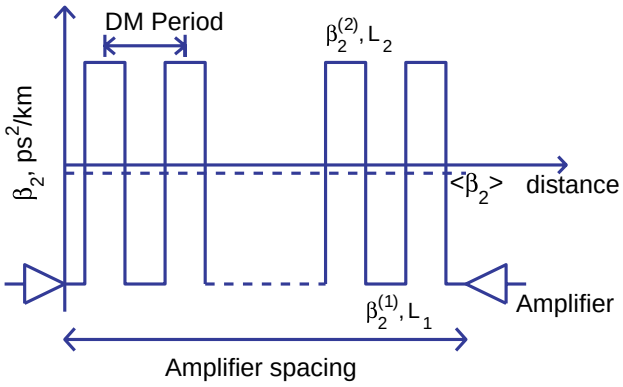

Figure 1. Schematics of a short period dispersion map with distributed amplification and bidirectional pumping.

dispersion $< d >$ and is given by

$$d(z) = \left| \begin{array}{ll} d_1 + < d > & \text{if} \quad 0 \leq Z \leq L/4 \\ d_2 + < d > & \text{if} \quad L/4 \leq Z \leq 3L/4 \\ d_1 + < d > & \text{if} \quad 3L/4 \leq Z \leq L \end{array} \right. , \tag{4}$$

where the normalized locally varying and the average dispersions are given by

$$d_j = -\frac{\beta_2^{(j)} L}{T_0^2}, \qquad < d >= -\frac{< \beta_2 > L}{T_0^2} = \frac{d_1 + d_2}{2} \tag{5}$$

The strength S of the dispersion map [7] is defined as

$$S = \left| \frac{\beta_2^{(1)} L_1 - \beta_2^{(2)} L_2}{T_{FWHM}^2} \right|, \tag{6}$$

where T_{FWHM} is the full width at half maximum of the soliton. In order to solve Eq. (3) we note that the self steepening and Raman effects are small enough to support stable DM solitons, and since these terms are small the right hand side of Eq. (3) can be treated as perturbation. In absence of the right hand side, Eq. (3) can be solved analytically using variational formulation [24]. This procedure has been widely used in nonlinear optics because of its simplicity and ability to predict fairly good results [23–27]. In order to solve unperturbed equation (3), we note that it can be solved using variation of the Lagrangian density Γ, such that

$$\delta \int_{-\infty}^{\infty} \int_{-\infty}^{\infty} \Gamma d\tau dZ = 0 \tag{7}$$

where the Lagrangian density Γ is given as [27]

$$\begin{aligned} \Gamma \; = \; & i \left(A \frac{\partial A^*}{\partial Z} - A^* \frac{\partial A}{\partial Z} \right) + d(Z) \left| \frac{\partial A}{\partial \tau} \right|^2 \\ & - G(Z)|A|^4 - i\mu \left(\frac{\partial^2 A}{\partial \tau^2} \frac{\partial A^*}{\partial \tau} - \frac{\partial^2 A^*}{\partial \tau^2} \frac{\partial A}{\partial \tau} \right) \end{aligned} \tag{8}$$

The unperturbed Schrödinger equation can be obtained by means of the functional derivative of Γ with respect to A, i.e.,

$$\frac{\delta \Gamma(A, A^*)}{\delta A^*} = 0 \tag{9}$$

The perturbed nonlinear Schrödinger equation i.e., the MNLSE as given by Eq. (3) can be easily recovered from the following relationship:

$$\frac{\delta\Gamma(A,A^*)}{\delta A^*} = iR[A,A^*] \tag{10}$$

In order to analytically estimate the periodic variation of pulse parameters in the dispersion managed system, it is convenient to postulate a simple Gaussian ansatz

$$A(Z,\tau) = \sqrt{\frac{E_0}{\sqrt{\pi}T(Z)}}\exp\left[-(1+iC(Z))\frac{(\tau-t_p(Z))^2}{2T^2(Z)} - i\Omega(\tau-t_p(Z)) + i\phi(Z)\right] \tag{11}$$

where E_0 is the normalised energy of the pulse, T is the pulse width, t_p is the position of pulse centre, C is the chirp, Ω is the nonlinear frequency shift and ϕ is the phase of the pulse. The peak amplitude $p(Z)$ of the pulse may be defined as $p(Z) = \sqrt{\frac{E_0}{\sqrt{\pi}T(Z)}}$. We now evaluate a finite dimensional reduced Lagrangian $L\left(T, t_p, C, \Omega, \phi, \frac{dT}{dZ}, \frac{dt_p}{dZ}, \frac{dC}{dZ}, \frac{d\Omega}{dZ}, \frac{d\phi}{dZ}\right)$ such that the evolution equations of pulse parameters are obtainable from $\delta \int_{-\infty}^{\infty} L dZ = 0$, where the reduced Lagrangian L is given by

$$\begin{aligned} L &= \int_{-\infty}^{\infty} \Gamma d\tau \\ &= \frac{2E_0}{T}\left(-\frac{T}{4}\frac{\partial C}{\partial Z} + \frac{C}{2}\frac{\partial T}{\partial Z} + \Omega T\frac{\partial t_p}{\partial Z} + T\frac{\partial \phi}{\partial Z}\right) \\ &\quad + \frac{d(Z)E_0}{T^2}\left(\frac{1+C^2}{2} + \Omega^2T^2\right) - \frac{G(Z)E_0^2}{\sqrt{2\pi}T} \\ &\quad + \frac{\mu E_0\Omega}{T^2}(3+3C^2+2\Omega^2T^2) \end{aligned} \tag{12}$$

Now the dynamical equations of different pulse parameters can be easily obtained using Euler Lagrange equation

$$\frac{d}{dZ}\left(\frac{\partial L}{\partial \dot{r}_j}\right) - \frac{\partial L}{\partial r_j} = 0 \tag{13}$$

where $r_j = T, C, t_p, \Omega$ and ϕ. At this stage perturbed variational procedure may be introduced to solve equation (3) with small but finite value of R. Since the MNLSE contains perturbation terms, therefore the modified Euler Lagrange equation can be written as [26]

$$\frac{d}{dZ}\left(\frac{\partial L}{\partial \dot{r}_j}\right) - \frac{\partial L}{\partial r_j} = i \int_{-\infty}^{\infty} \left(R\frac{\partial A^*}{\partial r_j} - R^*\frac{\partial A}{\partial r_j}\right) d\tau \tag{14}$$

By inserting the value of L from Eq. (12) in Eq. (14) we obtain a set of first order ordinary differential equations obeyed by pulse width parameters, which are as follows:

$$\frac{dT}{dZ} = -\frac{d(z)C}{T} + \frac{6\mu\Omega C}{T} \tag{15}$$

$$\frac{dC}{dZ} = -\frac{d(Z)(1+C^2)}{T^2} + \frac{G(Z)E_0}{\sqrt{2\pi}T} - \frac{6\mu\Omega(1+C^2)}{T^2} - \frac{E_0 G(Z)\varepsilon\Omega}{2\sqrt{2\pi}T} \tag{16}$$

$$\frac{\partial t_p}{\partial Z} = -d(Z)\Omega - \frac{3\mu}{2T^2}(1 + C^2 + 2\Omega^2 T^2) - \frac{3}{4}\frac{\varepsilon G(Z)E_0}{\sqrt{2\pi}T} \tag{17}$$

$$\frac{d\Omega}{dZ} = -\frac{E_0 G(Z)(\varepsilon C - T_R)}{2\sqrt{2\pi}T^3} \tag{18}$$

Additionally, the pulse amplitude $p(Z)$ and pulse width T are related to normalized pulse energy E_0 through $E_0 = \sqrt{\pi}p^2 T$, which is basically the energy conservation law. The solutions of equations (15)–(18) are required for finding the input pulse parameters T and C which ensure periodic pulse propagation in the DM system.

3. NUMERICAL EXPERIMENT AND RESULTS

In the present investigation, we consider the case where a Gaussian pulse is launched in a DM system with distributed amplification using bidirectional pumping scheme. The dispersion map consist of two fibers of equal length $L_1 = L_2 = L/2$, where $L = 4.216\,\text{km}$. Spacing between pumping station is $L_a = 29.5\,\text{km}$, i.e., 7 dispersion map in one pumping period. In the distributed amplification scheme that is the case considered in the present investigation, the transmission fiber is lightly doped with erbium ions and is pumped periodically from one or both directions, creating sufficient gain for compensating the fiber loss. Since the gain is distributed throughout the fiber links and compensates the fiber loss locally all along the fiber, soliton peak power variation in this system can be made much smaller as compared to a system with the lumped amplification scheme.

The most important criteria for designing soliton based transmission system with distributed amplification is to ensure that peak power varies as little as possible over each fiber span. Taking fibers with realistic attenuation $\alpha = 0.22\,\mathrm{dB/km}$, the net signal gain defined as $G(Z) = \exp\left(\int_0^z g(z)dz - \alpha z\right)$ over one fiber span is small. For such systems, soliton peak power varies less than 5% compared with original value. The resulting noise due to distributed amplification under such cases is also small. It is well documented [29] that bi-directional pumping causes small timing jitter. In fact, timing jitter in a DM system with distributed amplification and bi-directional pumping is not significantly different from the timing jitter caused in ideal distributed amplification for which losses are compensated by gain at every point. Thus, without sacrificing much accuracy, we focus on the case of ideal distributed amplification scheme in which local gain $g(Z) = \alpha$ at each point so that $G(Z) = 1$ in Eqs. (15)–(18). This simplification is usual and has been employed in many important investigations [29].

Before we take up numerical experiment, it is worth mentioning that, with the aid of full numerical simulation of MNLSE [30], it has been established that the interaction strength of neighbouring pulses is minimum when map strength $S = 1.65$. Therefore, while designing a DM system, in order to obtain optimum performance, we carefully select design parameters, particularly the length of the two types of fibers and their GVD value in such a way so as to achieve a map strength of $S \approx 1.65$. At this map strength the interaction strength of neighbouring pulses is minimum, this ensures better system performance. We first take a 100 Gb/s DM system operating at a wavelength $\lambda = 1.55\,\mu\mathrm{m}$. The required pulse width with a duty cycle of 4:1 is $T_{FWHM} = 2.5\,\mathrm{ps}$. We take typical fiber parameters $\beta_2^{(1)} = -2.4995\,\mathrm{ps^2/km}$, $\beta_2^{(2)} = 2.23926\,\mathrm{ps^2/km}$, $\beta_3 = -0.05\,\mathrm{ps^3/km}$, $\Gamma_R = 3\,\mathrm{fs}$ and $\alpha = 0.22\,\mathrm{dB/km}$ at the operating wavelength. For Gaussian input pulse $T_0 = T_{FWHM}/1.665 = 1.5\,\mathrm{ps}$. The calculated value of different parameters are as follows $< d >= 0.10$, $\mu = -0.0104$, $\varepsilon = 0.0006$, and $T_R = 0.002$. As initial condition we take Gaussian chirp free pulse ($C(0) = 0$). We now solve Eqs. (15)–(18) to find launching criteria of input pulses i.e., to find out appropriate value of pulse parameters such that T, C and E_0. We have launched the optical pulse at the chirp free point, which is the mid-point of an anomalous dispersion segment. At this point the pulse-width is minimum, and for convenience, at this point the normalized pulse width is taken as $T(0) = 1$, which corresponds to $T_{FWHM} = 2.5\,\mathrm{ps}$ for a 100 Gb/s transmission rate. We have allowed the pulse to propagate and applied the boundary conditions $T(0) = T(L)$ and $C(0) = C(L)$

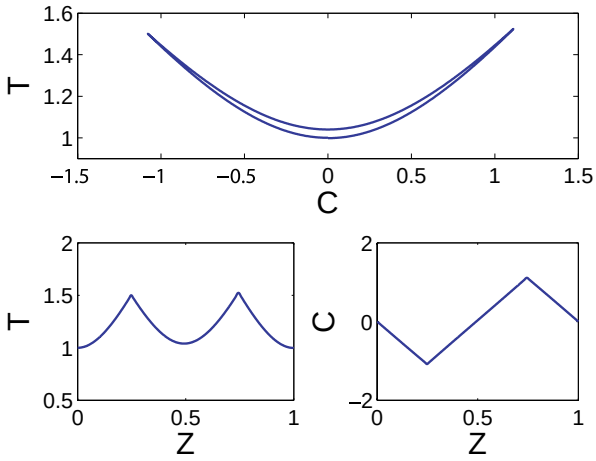

Figure 2. Evolution of pulse width and chirp within a DM cell. (a) Phase space trajectory of pulse width T and chirp C, (b) Variation of pulse width T with propagation distance Z, and (c) Variation of chirp C with propagation distance Z.

to find out appropriate value of E_0 by trail and error method. This estimated value of E_0 has been used for subsequent investigation. The normalized optimum peak power is obtained by dividing E_0 with $T(0)$.

Solutions of variational Eqs. (15)–(18) over one DM cell have been displayed in Figure 2. Pulse width T and chirp C produces a closed trajectory in the phase plane. Pulse width T is minimum at two ends of the DM cell. From Figure 2, it is evident that the variation of chirp with distance of propagation is linear. In the next step we use these solutions as input to the Eq. (3) and obtain full numerical solution of this equation. To obtain full numerical solution, we adopt well known split step Fourier method(SSFM) [23]. In this method the linear part has been solved using Fourier transform, while the nonlinear part has been solved using a fourth order Runge-Kutta algorithm for integration. The pulse has been allowed to propagate a distance of 4000 km during which no shading of radiation is visible. Under the influence of all the three higher order effects, namely, third order dispersion, intra-pulse Raman scattering and self steepening, the typical variation of the pulse shape within a single DM cell has been depicted in Figure 3. An example of the pulse dynamics of a solitary pulse over 4000 km is shown in Figure 4. It is noteworthy that although the higher order linear and nonlinear effects have been considered, the shape of the pulse remains unchanged and no distortion of pulse

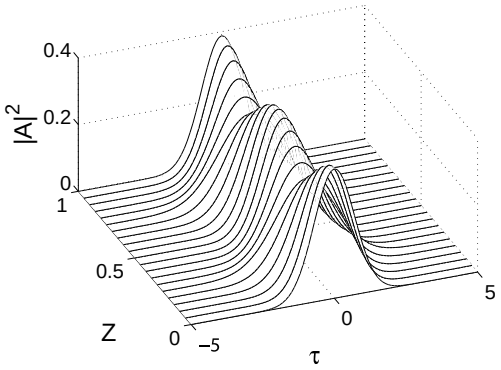

Figure 3. Pulse dynamics within a DM cell as obtained by full numerical simulation.

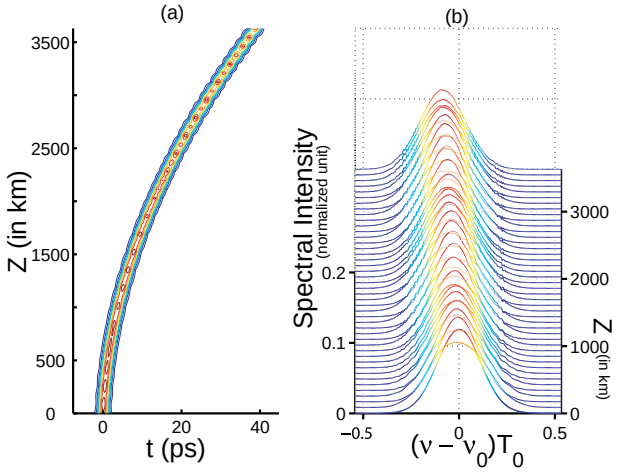

Figure 4. Propagation of a single pulse over a distance of 4000 km. $E_0 = 0.6875$, $T_{FWHM} = 2.5$ ps, $< d >= 0.10$. Map strength $S = 1.65$ (a) Temporal behaviour of the pulse. (b) Spectrum of the pulse.

shape has been identified. We have not noticed any asymmetrical broadening in the time domain due to third order dispersion. However, the phenomenon of self frequency shifts (SFS), owing to intra pulse Raman scattering has been clearly observed which resulting in slowing down the DM soliton. Therefore, as a result of this slowing down the central position of soliton shifts which is evident from Figure 4(a).

The variation of the soliton central position t_p with distance of propagation has been displayed in Figure 5. Both variational

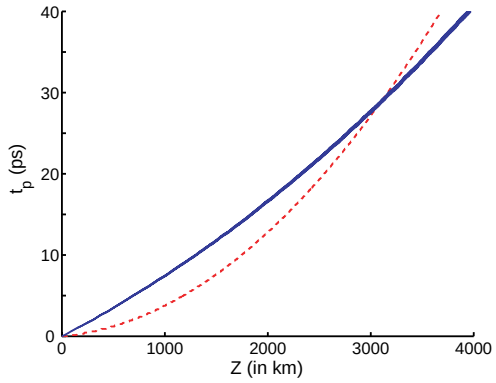

Figure 5. Variation of pulse centre t_p with propagation distance Z. Solid line obtained from solution of ODE's and broken line obtained from direct numerical simulation. $E_0 = 0.6875$, $T_{FWHM} = 2.5\,\text{ps}$, $< d >= 0.10$. Map strength $S = 1.65$.

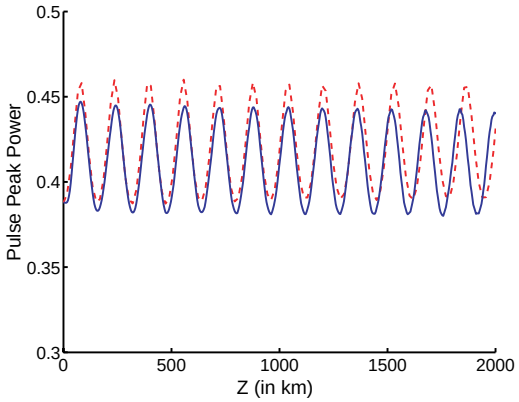

Figure 6. Variation of pulse peak power with propagation distance Z. Solid line for direct numerical simulation and dashed line for curve obtained from ODEs. Map strength $S = 1.65$.

and full numerical simulation results have been depicted. Results of variational formalism agree quite well with the results of full numerical simulations. We have examined the variation of t_p with dispersion and verified that it increases with the average dispersion, a known documented result. In Figure 6, the variation of normalised pulse peak power with propagation distance Z is shown for a distance of 2000 km. In figure the dashed line curve is obtained by solving variation

equations, whereas the solid line is obtained by solving equation (3) directly using SSFM. For both cases the value of the peak power has been noted down at the end of each DM cell where the pulse width is minimum as shown in Figure 2. Soliton energy E_0 is a very important parameter in any optical communication systems since it not only affects the interaction strength between neighbouring optical pulses but also affects signal to noise ratio. Variation of pulse energy E_0 with $< d >$ has been depicted in Figure 7. Pulse energy increases with the increase in the value of $< d >$.

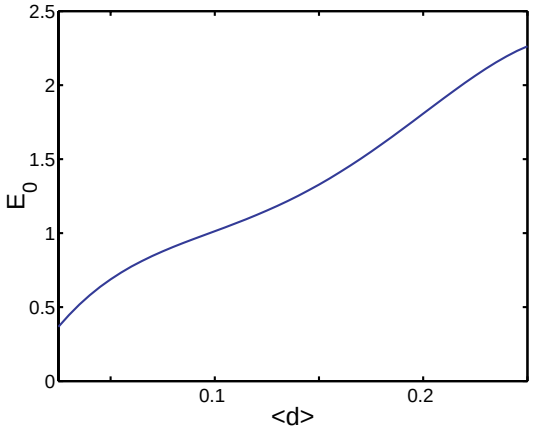

Figure 7. Variation of input pulse energy E_0 with average dispersion $< d >$. Map strength $S = 1.65$.

Pulse Interaction: After establishing that an isolated single pulse can travel large distance before being distorted or disintegrated, we turn our attention to study the nature of interaction between neighbouring pulses. We confine our attention to two cases, i.e., (i) interaction between two neighbouring pulses, and, (ii) interaction between a train of eight pulses. For both cases we take identical pulse with no initial phase difference. To study the nature of interaction we rely solely on numerical simulation of Eq. (3). However, the parameters of input pulses are decided from single soliton solution of ODE's given by Eqs. (15)–(18) and outlined earlier. We take following initial pulse profile:

$$A = \sqrt{\frac{E_0}{\sqrt{\pi}T}} \sum_{i=1}^{N} \left[\exp\left(\frac{(\tau - (2i-1)t_p)^2}{2T^2} \right) + \exp\left(\frac{(\tau + (2i-1)t_p)^2}{2T^2} \right) \right] \tag{19}$$

where $N = 1$ for two solitons interaction and $N = 4$ for eight solitons

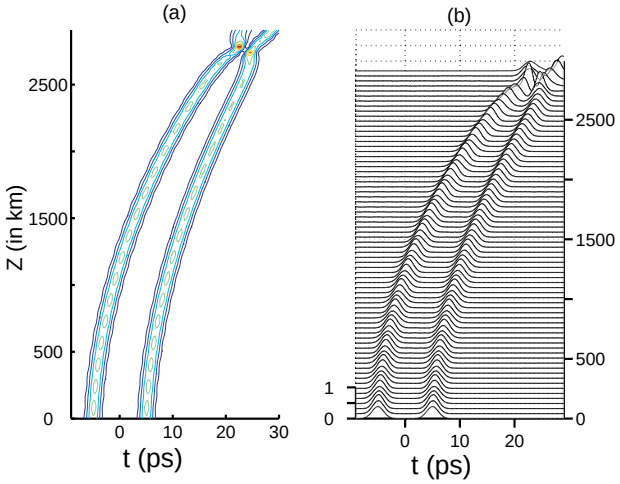

Figure 8. Interaction of two identical in phase neighbouring pulses. Transmission speed 100 Gb/s. For each pulse $E_0 = 0.6875$. $< d >= 0.10$(a) Contour plot, (b) Mesh plot. Map strength $S = 1.65$.

interaction. For 100 Gb/s transmission speed the peak-to-peak pulse separation in natural units is $2t_p = 10$ ps. Figure 8 displays an example of the intra-channel interaction between two DM solitons in the SPDM system, whereas Figure 9 demonstrates interaction among pulses in the 8 bit pulse train. We have repeated our numerical experiments for different values of $< d >$ and noted down the collision distance between neighbouring pulses for different cases. The collision distance for the 8 bit pulse train is taken as the distance at which any two neighbouring pulses of the train collapse. The variation of collision distances with the average dispersion $< d >$ for two and eight pulses has been displayed in Figure 10. In this figure, the solid line represents two soliton interactions and dashed line represents eight solitons interaction. It is evident from the figure that for both two and eight pulses soliton propagation the interaction length is larger for smaller value of $< d >$. Hence, very large value of $< d >$ should be avoided during system design. It is noteworthy from Figure 10 that the collision distance for the train of eight pulses is larger in comparison to collision distance for two pulses. In addition, two outer member of the pulse train collide earlier than any two inner member of the pulse train. This may be attributed to the fact that, for a pulse, which is located inside, the train the presence of pulses in both sides of the time domain produce symmetrical attractive interaction force, i.e., the pulse experiences

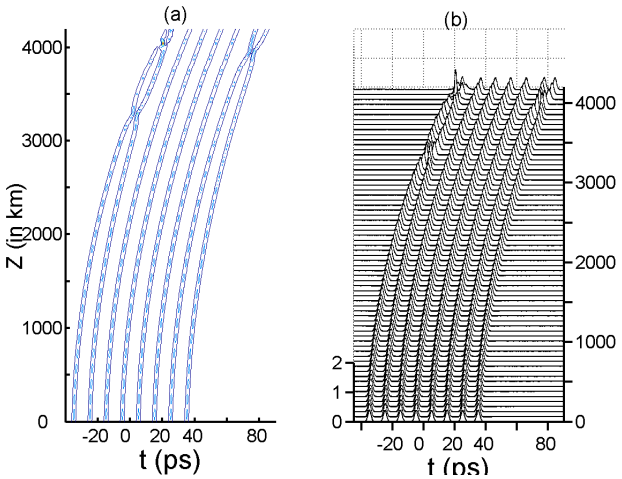

Figure 9. Interaction of eight identical in phase DM soliton pulses. Transmission speed 100 Gb/s. For each pulse $E_0 = 0.6875$. $< d >= 0.10$ (a) Contour plot, (b) Mesh plot. Map strength $S = 1.65$.

attractive force both in the front and tail portion. Thus, since pulses from both sides attract with equal force thereby effectively reducing the collision distance. Whereas, for a pulse in the outer region of the train, interaction force is asymmetric resulting in early collision. This argument is also applicable for the case of a pair of pulses.

We now proceed to examine the roles played by higher order linear and nonlinear effects. We allow two and eight pulses to propagate down the system and switch off all higher order terms from the MNLSE. The behaviour of pulse dynamics for 100 Gb/s system is shown in Figure 11. It has been estimated that in comparison to the case where all the three higher order perturbation terms are present, in the present case the collision length for two interacting neighbouring pulses reduces approximately 7%, whereas the reduction in collision length for eight interactions is only 4%. The behaviour of pulse dynamics for an 110 Gb/s and 120 Gb/s system have been respectively shown in Figs. 12 and 13. Intra-pulse collision distance at different transmission rate has been depicted in Fig. 14. From figure it is evident that higher order effects have negligible influence on intra-pulse collision distance. We have confirmed that the change in collision distance due to higher order effects is less than 4% for transmission rate higher than 100 Gb/s. This is due to the fact that at still higher transmission rate the initial intra-pulse distance is very small and these intra-pulse separations mainly determine the collision distance, the higher order linear and nonlinear

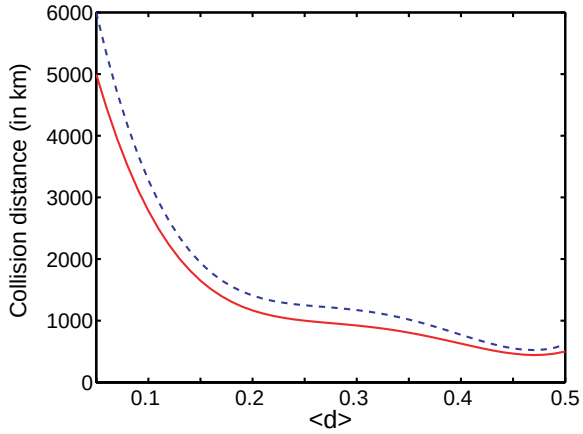

Figure 10. Variation of collision distance with average dispersion $< d >$. Solid line for two soliton interaction and dashed line for eight soliton interaction. Transmission speed 100 Gb/s. Map strength $S = 1.65$.

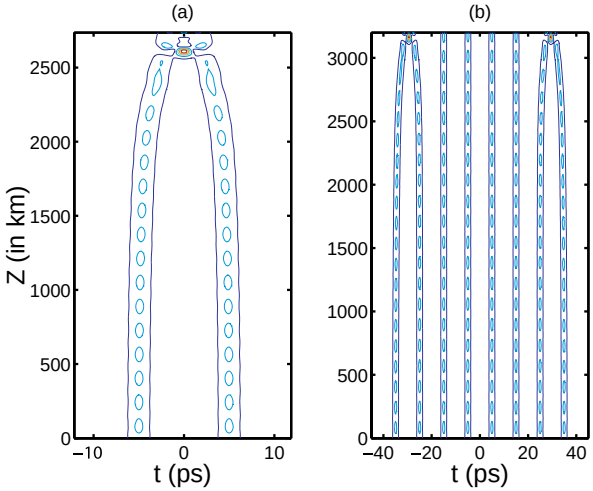

Figure 11. Pulse dynamics at 100 Gb/s without intra-pulse Raman scattering, self steepening and third order dispersion. (a) Interaction of two pulses, (b) interaction of eight identical pulses. For each pulse $E_0 = 0.6875$. Map strength $S = 1.65$.

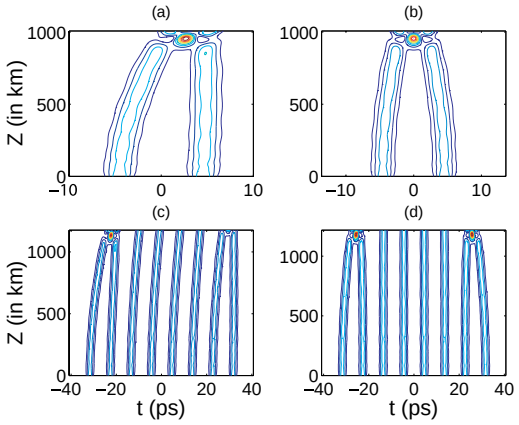

Figure 12. Pulse dynamics at 110 Gb/s with $< d >= 0.10$. Each pulse is identical with energy $E_0 = 0.6875$ Upper panel is for two pulses, whereas the lower panel is for a train of eight identical pulses. subplot (a) and (c) are without intra-pulse Raman scattering, self steepening and third order dispersion. Subplot (b) and (d) are with intra-pulse Raman scattering, self steepening and third order dispersion. Map strength $S = 1.65$.

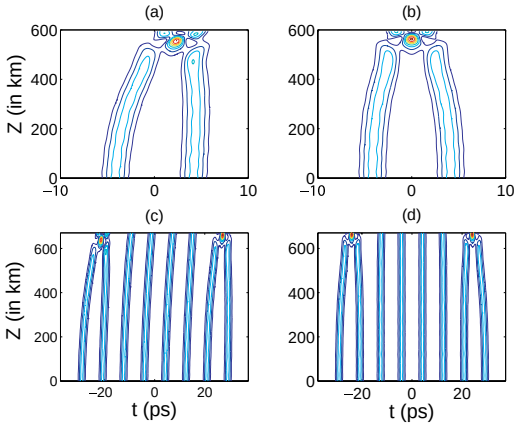

Figure 13. Pulse dynamics at 120 Gb/s with $< d >= 0.10$. Each pulse is identical with energy $E_0 = 0.6875$ Upper panel is for two pulses, whereas the lower panel is for a train of eight identical pulses. subplot (a) and (c) are without intra-pulse Raman scattering, self steepening and third order dispersion. Subplot (b) and (d) are with intra-pulse Raman scattering, self steepening and third order dispersion. Map strength $S = 1.65$.

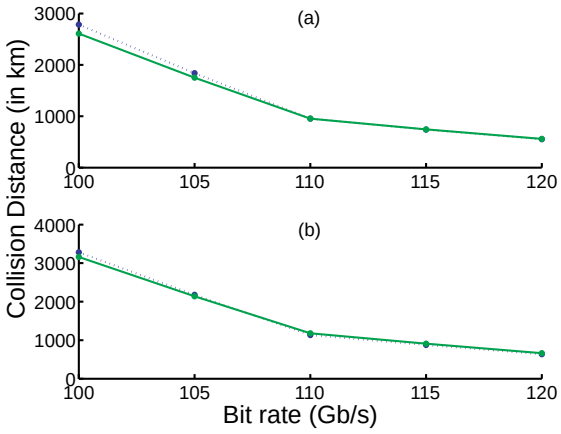

Figure 14. Variation of intra-pulse collision length with transmission speed. Solid line represents a case when third order dispersion, self steepening and Raman scattering is absent. Dotted line represents the case when all three higher order terms are present. (a) Two pulses. (b) Eight pulses. Map strength $S = 1.65$.

phenomena have only marginal influence on intra-pulse interaction in dense dispersion managed systems.

4. CONCLUSION

In this paper we have investigated optical pulse propagation in a high bit rate dense dispersion managed(DM) optical communication system operating at the speed of 100 Gb/s and more taking into account of the effects of third order dispersion, intra-pulse Raman scattering and self steepening. Using perturbed variational formulation, we have obtained several ordinary differential equations for various pulse parameters. These equations have been solved numerically to identify launching criteria in the first DM cell of the system. Full numerical simulation of the nonlinear Schrödinger equation has been undertaken to identify effects of higher order terms on pulse propagation and to investigate the intra-pulse interaction. For a 100 Gb/s system, it has been found that the shift of the pulse centre due to intra-pulse Raman scattering increases with the increase in the distance of propagation and average dispersion. We have noticed that for higher value of average dispersion pulses travel less distance before collision than for lower average dispersion, thus large value of $< d >$ is detrimental to long distance propagation.

ACKNOWLEDGMENT

This work is supported by the Department of Science and Technology (DST), Government of India, through the R&D grant SP/S2/L-21/99 and the support is acknowledged with thanks.

REFERENCES

1. Smith, N. J., F. M. Knox, N. J. Doran, K. J. Blow, and I. Bennion, "Enhanced power soliton in optical fibers with periodic dispersion," *Electron. Letts.*, Vol. 32, 54, 1996.
2. Mishra, M. and S. Konar, "Interaction of solitons in a dispersion managed optical communication system with asymmetric dispersion map," *J. Electromagn. Waves and Appl.*, Vol. 21, 2049, 2007.
3. Turitsyn, S. K. and E. G. Shapiro, "Disperson managed soliton in optical amplifier transmission systems with zero average dispersion," *Optics Letts.*, Vol. 23, 682, 1998.
4. Carter, G. M., J. M. Jacob, C. R. Menyuk, E. A. Golovehenko, and A. N. Pilipetski, "Timing jitter reduction for a dispersion managed soliton systems: experimental evidence," *Optics Letts.*, Vol. 22, 513–515, 1997.
5. Grigoryan, V. S. and C. R. Menyuk, "Dispersion-managed soliton at normal average dispersion," *Opt. Letts.*, Vol. 23, 609, 1998.
6. Biswas, A., S. Konar, and E. Zerrad, "Soliton-soliton interaction with parabolic law nonlinearity," *Journal of Electromagnetic Waves and Applications*, Vol. 20, 927, 2006.
7. Berntson, A., D. Anderson, N. J. Doran, W. Forysiak, and J. H. B. Nijhof, "Power dependence and accessible bandwidth for disperson-managed solitons in asymmetric disperson maps," *Electron. Letts.*, Vol. 34, 2054, 1998.
8. Berntson, A., N. J. Doran, W. Forysiak, and J. H. B. Nijhof, "The power dependence of dispersion managed solitons for anomalous, zero, and normal path-average dispersion," *Opt. Letts.*, Vol. 23, 900, 1998.
9. Konar, S., J. Kumar, and P. K. Sen, "Suppression of soliton instability by higher order nonlinearity in long haul optical communication systems," *J. Nonlinear Optical Physics and Materials*, Vol. 8, 497, 1999.
10. Crutcher, S., A. Biswas, M. D. Aggarwal, and M. E. Edwards, "Oscillatory behaviors of spatial solitons in two-dimensional waveguides and stationary temporal power solitons in optical

fibers," *Journal of Electromagnetic Waves and Applications*, Vol. 20, 761, 2006.

11. Ballav, M. and A. R. Chowdhury, "On a study of diffraction and dispersion managed soliton in a cylindrical media," *Progress In Electromagnetics Research*, PIER 63, 33, 2006.
12. Biswas, A. and S. Konar, "Theory of dispersion-managed optical solitons," *Progress In Electromagnetics Research*, PIER 50, 83, 2005.
13. Shwetanshumala, S., A. Biswas, and S. Konar, "Dynamically stable super-gaussian solitons in semiconductor doped glass fibers," *Journal of Electromagnetic Waves and Applications*, Vol. 20, 901, 2006.
14. Kurtz, K., "Suppression of fiber nonlinearity by appropriate dispersion management," *IEEE Photonics Technology Letts.*, Vol. 5, 1250, 1993.
15. Tkach, R. W., A. R. Chraplyvy, F. Forghieri, A. H. Gnanck, and R. M. Derosier, "4-photon mixing and high speed WDM systems," *J. Lightwave Technolo.*, Vol. 13, 841, 1995.
16. Smith, N. J., W. Forysiak, and N. J. Doran, "Reduced Gordon Haus jitter due to enhanced power solitons in strongly dispersion managed system," *Electronics Letts.*, Vol. 32, 2085, 1996.
17. Hasegawa, A. and Y. Kodama, "Guiding centre solitons in optical fibers," *Optics Letts.*, Vol. 15, 1443, 1990.
18. Kodama, Y., A. Maruta, and A Hasegawa, "Long distance communications with solitons," *Quantum Optics*, Vol. 6, 463, 1994.
19. Hirooka, T., T. Nakada, and A. Hasegawa, "Feasibility of densly dispersion managed soliton transmission at 160Gb/s," *IEEE Trans. Photonics Tech. Letts.*, Vol. 12, 633, 2000.
20. Richardson, L. J., W. Forysiak, and N. J. Doran, "Dispersion managed solitons propagation in short period dispersion maps," *Optics Letts.*, Vol. 25, 1010, 2000.
21. Maruta, A., Y. Yamamoto, S. Okamoto, A. Suzuki, T. Morita, A. Agata, and A. Hasegawa, "Effectiveness of densly dispersion managed solitons in ultrahigh speed transmission," *Electron. Letts.*, Vol. 36, 1947, 2000.
22. Tchofo Dinda, P., A. B. Moubissi, and K. Nakkeeran, "Collective variable theory for optical solitons in fibers," *Phys. Rev. E*, Vol. 64, 016608, 2001.
23. Agrawal, G. P., *Nonlinear Fiber Optics*, Academic Press, San Diego, 1995.

24. Anderson, D., "Variational approach to nonlinear pulse propagation in optical fibers," *Phys. Rev. A*, Vol. 27, 3135, 1983.
25. Konar, S. and S. Jana, "Linear and nonlinear propagation of sinh-Gaussian pulses in dispersive media possessing Kerr nonlinearity," *Optics Communication*, Vol. 236, 7, 2004.
26. Biswas, A., "Dispersion managed solitons in optical fibers," *J. Opt. A: Pure Appl. Opt.*, Vol. 4, 84–97, 2002.
27. Mookherjee, S. and A. Yariv, "Hamiltonian dynamics of breathers with third order dispersion," *J. Opt. Soc. Am. B*, Vol. 18, 1150–1155, 2001.
28. Liao, Z. M. and G. P. Agrawal, "High bit rate soliton transmission using distributed amplification and dispersion management," *IEEE Photonics Tech. Letts.*, Vol. 11, 818, 1999.
29. Poutrina, E. and G. P. Agrawal, "Timing jitter in dispersion managed soliton systems with distributed, lumped and hybrid amplification," *J. Lightwave Technol.*, Vol. 29, 790, 2002.
30. Yu, T., E. A. Glovchenko, A. N. Pilipetski, and C. R. Menyuk, "Dispersion managed soliton interactions in optical fibers," *Opt. Letts.*, Vol. 22, 793, 1997.